J. Biomechanics Vol. 19, No. 5, pp. 385–397, 1986.
Printed in Great Britain

0021-9290 86 $3.00 + .00
Pergamon Journals Ltd.

COSSERAT MICROMECHANICS OF HUMAN BONE: STRAIN REDISTRIBUTION BY A HYDRATION SENSITIVE CONSTITUENT

H. C. PARK and R. S. LAKES*
Department of Biomedical Engineering ~~and Department of Mechanical Engineering,~~ Engineering Physics
~~[illegible], U.S.A.~~
University of Wisconsin, Madison

Abstract—Experimental determination of the strain distribution in prismatic, square cross-section bars of human compact bone in torsion disclosed nonclassical effects associated with the microstructure. Specifically, in wet bone at small strain, significant deviations from the classically predicted strain distribution were observed. The measured strain distribution in wet bone followed predictions based on Cosserat (micropolar) elasticity. In dry bone, the strain distribution was very close to the prediction of classical elasticity. The interaction between Haversian osteons and the cement substance between them was hypothesized to be the principal mechanism for the phenomena. To evaluate this hypothesis, additional specimens were subjected to prolonged torsional load and the cement lines were observed by reflected light microscopy. Localized deformation at the cement lines was observed, but it was less than values reported earlier for bovine plexiform bone.

NOMENCLATURE

a	dimension of side of square cross section prism
d	osteon diameter
dF	differential increment of force on an area element
dM	differential increment of moment on an area element
e_{zy}	tensorial shear strain
G	shear modulus
$J(t)$	creep compliance as a function of time
J_0	compliance used to normalize creep results
l_b	Cosserat characteristic length, bending
l_t	Cosserat characteristic length, torsion
M	twisting moment
N	Cosserat coupling number
u	displacement at cement line
θ	twist angle per unit length

INTRODUCTION

Bone tissue is a complex composite material which at different levels of scale exhibits fibrous, porous, and particulate microstructural features. Several aspects of the role of the bony microstructure have been elucidated via composite theory by Bonfield and Grynpas (1977) and by Katz (1980). While understanding of bone as a classically elastic composite has been gained, other characteristics of its behavior remain poorly understood. In particular, bone fracture in the presence of stress raisers such as holes or notches does not follow the predictions of classical elasticity. In the case of holes, Brooks *et al.* (1970) found the stress concentration factor for fracture to be significantly less than the predicted value. In the case of controlled notches, Bonfield and Datta (1976) observed that the strength did not depend on the root radius r of the notch in the expected way, i.e. strength proportional to $\sqrt{r}$. Instead, the strength was found to be almost independent of root radius. These observations cannot be attributed solely to nonlinear and/or irreversible processes which may occur as fracture is initiated, for the following reasons. Lakes and Yang (1983a) found that under conditions of small strain and linear behavior, the distribution of strain around a circular hole in a strip of bone under tension differed from predictions based on classical anisotropic elasticity. The maximum concentration of strain was less than the classically predicted value; strain was found to be redistributed into regions which were expected classically to experience a relatively small strain. Wright *et al.* (1977), in studies of residual stress in bone via the hole drilling method, found behavior at variance with the predictions of classical anisotropic elasticity. Stresses observed in this study were well within the range for linear behavior. Carter *et al.* (1981) observed that the fatigue life of bone specimens in bending exceeds that of specimens in tension by a factor of several thousand. These results all point up the limitations of classical elasticity theory as a continuum model for bone at stresses below the yield point.

Recent evidence of Cosserat (i.e. micropolar) elasticity in bone obtained by Yang and Lakes (1981, 1982) and by Lakes (1981) may account for some of the above discrepancies. Cosserat elasticity is a generalized continuum theory (Eringen, 1968) which admits degrees of freedom in addition to those present in classical theory, i.e. translation of points and force per unit area (stress). There is an extra kinematical degree of freedom, a local rotation of points, and an extra dynamical degree of freedom, couple stress, i.e. a torque per unit area. These degrees of freedom are thought to be associated with motions of and forces upon structural elements in composites and other structured materials. The constitutive equations for a Cosserat elastic solid are given in Appendix A. Six

Received July 1985; in revised form November 1985.
*Author to whom correspondence should be addressed.

elastic constants are required for an isotropic Cosserat solid compared with two for an isotropic classical solid. Various combinations of the new elastic constants have physical significance. In particular, the characteristic lengths defined in Appendix A have dimensions of length and have been theoretically shown (Askar and Cakmak, 1968) to be of the order of the size scale of structural elements of simple microstructures.

Cosserat solids are predicted to behave differently in a variety of ways from classical solids. In the context of bone mechanics perhaps the most significant of these predictions are that Cosserat solids exhibit less concentration of stress and strain around circular holes (Cowin, 1970), around elliptic holes (Kim and Eringen, 1973) and around cracks (Ejike, 1969) than expected classically. It is also predicted that the size dependence of rigidity of Cosserat solids in various torsion and bending geometries differs from classical predictions. Specifically, the rigidity is predicted to exceed classical values in specimens which are thin. Experiments aimed at the determination of Cosserat elastic constants have been designed on the basis of these predictions. Plate bending experiments upon metals by Ellis and Smith (1968) and by Schijve (1966) revealed purely classical behavior as did torsional size effect measurements by Gauthier and Jahsman (1975). Cosserat elastic behavior was observed in bone in torsional and bending size effect studies upon circular cylindrical specimens by Yang and Lakes (1981, 1982). Recently the method of size effects was applied to an isotropic polymer foam to determine all six of its Cosserat elastic constants (Lakes, 1986). The method is, however, tedious since a set of cylindrical specimens of different diameter must be prepared.

The purposes of the present study are to examine micromechanical effects in bone in new geometries, to test the predictive power of Cosserat elasticity for bone and to explore the microstructural mechanisms which may be responsible for Cosserat elastic behavior in bone. Experiments were performed to (1) determine the distribution of strain on the lateral surfaces of prismatic, square cross-section bars of wet and dry bone in torsion, and to (2) determine the distribution of microdisplacement at the cement lines in similar specimens loaded for prolonged periods.

The theoretical basis for the design and interpretation of the experiments lies in an analytical solution for the torsion of a square cross-section prism of a Cosserat elastic material (Park and Lakes, in press), reproduced in part in Appendix B. The solution predicts that the shear strain distribution across the lateral surfaces will differ from the classical prediction, depending on the Cosserat elastic constants of the material. In particular, a nonvanishing shear strain can occur at the corners of the cross-section, in contrast to the case of classical elasticity.

Additional experiments were designed to explore possible mechanisms for Cosserat elastic behavior in bone. The experiments were based on the observation of Lakes and Saha (1979) that shear strain in bovine plexiform bone under creep conditions was due to localized motion at the interface between the laminae. In the present study the cement lines between osteons of human Haversian bone were examined to determine: (1) whether localized interfacial motion also occurred in human bone and (2) whether such motion could constitute a mechanism for Cosserat mechanics in bone. It was intended that cement line displacements be measured as a function of position across the lateral surface of specimens and as a function of time in creep, and that the time dependent microdisplacements be compared with the macroscopic creep.

The hypothetical microdisplacement distribution is shown in Fig. 1. A prism made of a classically elastic continuum is shown in Fig. 1a. In the classical case the cross-sections undergo warp and the strain vanishes at the corners of the cross-section. A fibrous prism is shown in Fig. 1b. The matrix between the fibers is assumed to be a thin layer, much more compliant than the fibers. The continuum counterpart of this fibrous prism is embodied in the Cosserat elastic solution outlined in Appendix B. The mathematical rationale for treating a fibrous structure as a Cosserat-type continuum has been presented in the generalized composite theories of Hlavacek (1975), Achenbach (1976) and Malcolm (1982). The physical rationale, indicated in Fig. 1b, is that each fiber can support a moment as well as a force; in a continuum approximation the average moment per unit area becomes the couple stress. If the matrix between the fibers is viscous or viscoelastic, the microdisplacement distribution can be expected to be time-dependent. The corresponding continuum representation becomes Cosserat viscoelasticity (Eringen, 1977), a relatively straightforward extension of the elastic theory.

MATERIALS AND METHODS

Specimens of human compact bone were obtained from the femoral cortex of a donated cadaver from a 62 yr old male. They were stored without preservatives or fixatives in a freezer. Laboratory specimens were prepared by rough cutting on a bandsaw and were then machined slowly while wet, on a milling machine, into prismatic bars with a square cross-section. Machining was done with a tool steel end mill 6.1 mm in diameter, rotating at 500 revolutions min^{-1}, under water irrigation. The long axis of each specimen was parallel to the bone axis. The specimens were then subjected to quasistatic torsional load in two kinds of experiments described below.

Strain distribution

The strain distribution across the lateral surface of prismatic square cross-section bars of bone *ca.* 6 mm wide in torsion was determined using strain gages. A specimen of commercially pure polymethyl methacrylate (PMMA) was also examined as a control. Each specimen was air dried and 120 Ω strain gages

were glued on the lateral surfaces with cyanoacrylate adhesive. These strain gages had a gage length of 0.2 mm, sufficiently small in the present experiments to minimize errors due to averaging in the presence of strain gradients. Four pairs of strain gages were applied at different locations on the surface; in each pair one gage was oriented 45° and the other was 135° from the long axis of the specimen, as shown in Fig. 2 This configuration permitted the determination of the shear strain distribution due to torsion. The angle of each strain gage was measured using a Kodak contour projector and its position was measured using a calibrated microscope. The effect of errors in the strain gage angle were judged to be small based on the rosette analysis of Perry and Lissner (1962) in which a 2° angulation error was predicted to result in a strain error of 2%. A parasitic bending deformation in response to torsional load is possible in bone if its material axes are slightly misaligned with respect to the specimen long axis. Two additional strain gages of gage length 0.79 mm were therefore cemented parallel to the longitudinal direction to measure parasitic bending. Readings from these gages were used to perform fine adjustments of the loading system to minimize parasitic bending. Due to the poor thermal conductivity of bone and the small size of the gages, a small excitation voltage of 0.2 V was used to prevent error due to overheating of the strain gages. Each end of the specimen was machined to a flat surface perpendicular to the specimen axis. Screws were then glued to both ends of the specimen with cyanoacrylate adhesive and it was mounted in a torsion apparatus similar to that described by Yang and Lakes (1981, 1982). Step torque of known magnitude was applied by means of an arrangement of dead weights and low-friction, ball bearing pulleys. The risetime was less than 1 s and the torque was maintained for 60 s. Twist angle was determined by measurements of the angular displacements of laser beams reflected from two mirrors attached to the specimen. Each mirror was *ca.* 6 mm square and was mounted on a stalk fixed to the specimen at one point with cyanoacrylate adhesive. This differential approach eliminated the contribution of any end effects due to the restriction of the warp of the square cross-sections by the mounting. Effects of the compliance of the mounting cement were similarly eliminated. Data were taken 10 s after application of the torque. These strain distribution experiments were performed upon dry bone, wet bone and polymethyl methacrylate (PMMA).

Analysis of the strain distribution data and comparison with theory were conducted as follows. Strain gage data were converted to the tensorial shear strain element e_{zy} and were normalized by dividing by the twist angle per unit length and by the width of the specimen. Theoretical strain distributions based on classical elasticity (Timoshenko and Goodier, 1983) and on Cosserat elasticity (Park and Lakes, in press) were computed for comparison with the experimental results. In classical elasticity, the normalized strain

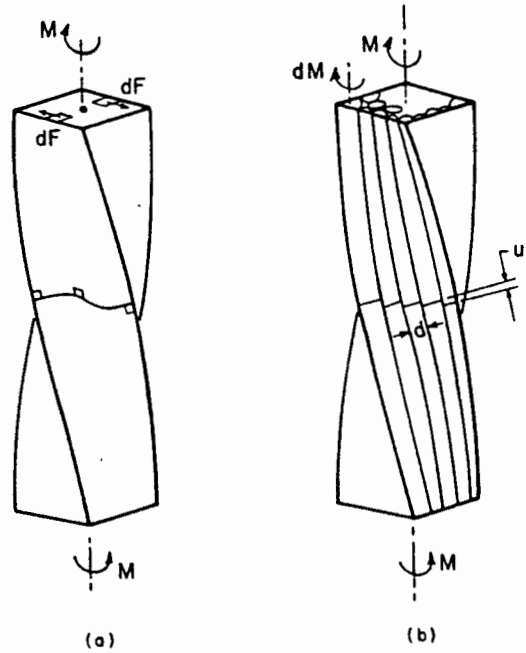

Fig. 1. Warp and strain due to torsion. (a) Classically elastic homogeneous prism (b) Fibrous prism.

distribution is independent of the elastic constants, but in Cosserat elasticity, the distribution depends on the elastic constants. Cosserat elastic constants were obtained for human compact bone by the 'method of size effects' in which the size dependence of bending and torsional rigidity of circular cylinders was used to infer the elastic constants. Elastic constants (see Appendix A) used for comparison with theory in the present study were: $l_t = 0.2$ mm, $G = 4.5$ GPa, $\psi = 1.5$, $N = 0.9$ and $l_b = l_t/\sqrt{3}$. The shear modulus G does not influence the predicted normalized strain distribution. The values of l_t were found by Yang and Lakes (1981) and were confirmed by Lakes and Yang (1983b). Regarding l_t observe that there are several definitions (Mindlin and Tiersten, 1962) which differ by a multiplicative constant. The definition of the torsional characteristic length l_t used here is due to Gauthier and Jahsman (1975). Regarding the coupling number N, the experiments of Yang and Lakes (1981) were consistent with $N = 1$ but did not determine N accurately due to limitations on the range of specimen sizes studied. Further experiments with bone microsamples by Lakes and Yang (1983b) indicated $N \geqslant 0.5$ and were consistent with $\psi = 1.5$. In the present study, a value of $N = 0.9$ was used to generate the theoretical curves. Regarding l_b, in the square prism geometry for torsion, the characteristic length for bending l_b enters in the analysis, by contrast to the circular cylinder geometry (Gauthier and Jahsman, 1975) in which l_t is the only characteristic length involved. Since bone is anisotropic, the l_b value from the bending study of Yang and Lakes (1982) is not relevant to the present situation. In the present study, it was assumed that $l_b = l_t/\sqrt{3}$, corresponding to $\beta/\gamma = 0.5$. The rationale

for this is that strain distributions predicted analytically by Park and Lakes (in press) were not very sensitive to l_b/l_t, so that the assumption of a particular value of l_b should not be problematical.

Microdisplacement distribution

Specimens of compact bone were cut in the wet state into prisms 19 mm long and 3.2 mm by 3.2 mm in square cross-section, and with cylindrical ends. The flat lateral surfaces were wet-polished with graded abrasives to permit examination of the specimen by reflected-light microscopy. Fiduciary marks were made by orienting a razor edge perpendicular to the bone axis and pressing it to the specimen surface. Prior to loading, these marks were verified as straight by examining the specimen under a reflected-light microscope. Specimens were kept immersed in Ringer's solution before and during the experiments. Temperature was maintained constant by means of a closed loop temperature controller. A temperature of 37°C (human body temperature) was used during the initial experiments. Based on the observation of Lakes *et al.* (1979) that increased temperatures result in accelerated viscoelastic deformation in bone, further creep tests were conducted at 50°C. Torsional loading was applied within a 1 s rise-time by means of an arrangement of weights and pulleys, and the load was held constant for the duration of the test. The specimen angular displacement was found by measuring the linear displacement of an arm fixed to the rotor shown in Fig. 3 via a micrometer barrel capable of resolving 0.0001 in. (2.5 μm). A bacteriostatic agent was added to the Ringer's solution to prevent decay of specimens during lengthy experiments. Loss of water via evaporation from the warm Ringer's solution was replenished by continuously siphoning distilled water into the specimen chamber through a fine tubule. Creep deformation was measured at two different loads for each specimen; one creep test was done under small load, resulting in 0.05–0.08% initial maximum nominal shear strain (calculated using classical elasticity theory) and the other at 0.6–1.2% initial maximum shear strain. Sufficient time was allowed for recovery following the first creep test. The 'small' load corresponds to the upper bound on stresses routinely encountered in humans in normal activities: *in vivo* studies disclosed that the peak principal tensile and compressive strains in the anterior tibia of a walking man are 0.0341% and −0.0425%; for jogging the corresponding values are 0.0847% and −0.0578% (Lanyon *et al.*, 1975). For the small load, creep was measured from 10 s up to 49 days and for the large load, up to 131 days. Specimens were observed during creep with a reflected light microscope as shown in Fig. 3 in order to evaluate the time evolution of the microdisplacement distribution as described above; the specimens were also examined at the conclusion of each creep test. Photomicrographs were taken following these visual observations. Cement line displacements were measured at several locations on the micrographs by setting up an imaginary center line of the fiduciary marks and measuring the shift of the center line of the mark at the cement line; each location was measured three times.

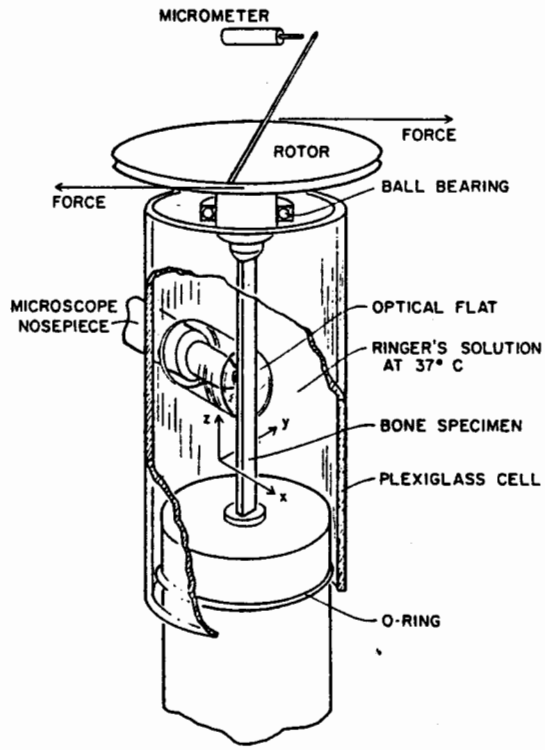

Fig. 3. Experimental configuration for creep and cement line studies. Rotation of the top rotor was measured by advancing the micrometer screw until it contacted the arm; contact was ascertained by measuring electrical continuity.

RESULTS

Strain distribution

Results are shown in Figs 4–6. Figure 4 displays results for wet and dry bone. This specimen was tested first when dry, then it was kept in a humid environment for 5 days and immersed in water for 10 h. The dry bone behaved essentially classically, while the same specimen while wet behaved as a Cosserat solid. Another specimen was measured while dry and submerged immediately in water for 12 h; results are shown in Fig. 5. Conditions of intermediate hydration were also explored: a third specimen was measured after it was wrapped in a wet cloth for 2 days and for 4 days, as shown in Fig. 6. The PMMA, examined as a control, behaved according to classical predictions.

Microdisplacement distribution

A total of eight specimens were subjected to creep tests under two different temperature conditions (37°C, 50°C) as shown in Table 1. As indicated in this table, each specimen was also subjected to a preliminary creep test at body temperature and at a relatively small torque. Comments indicate reasons for

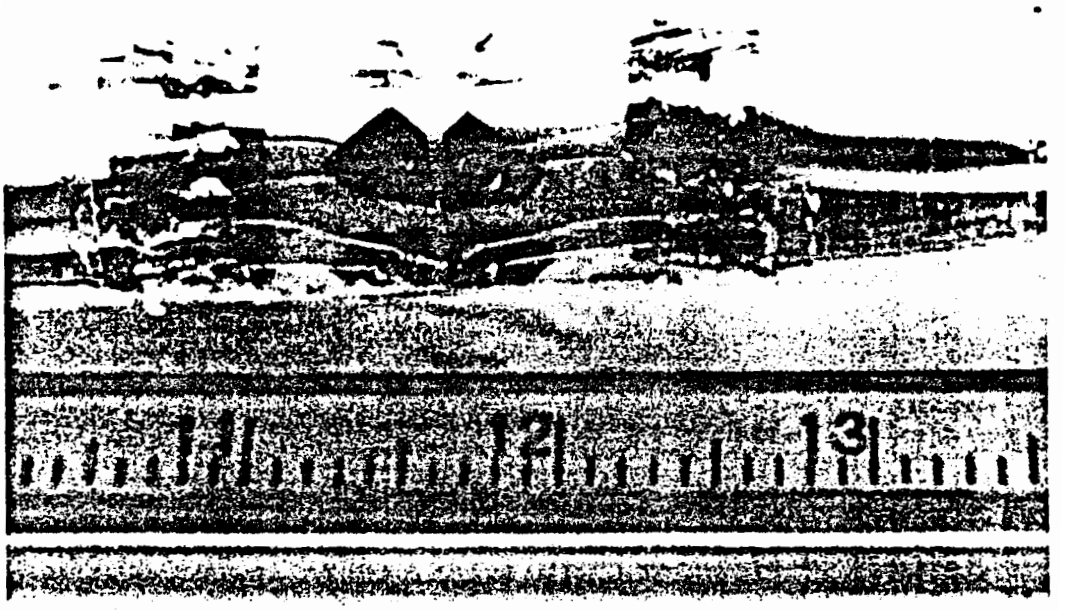

Fig. 2. Specimen with strain gages; metric scale.

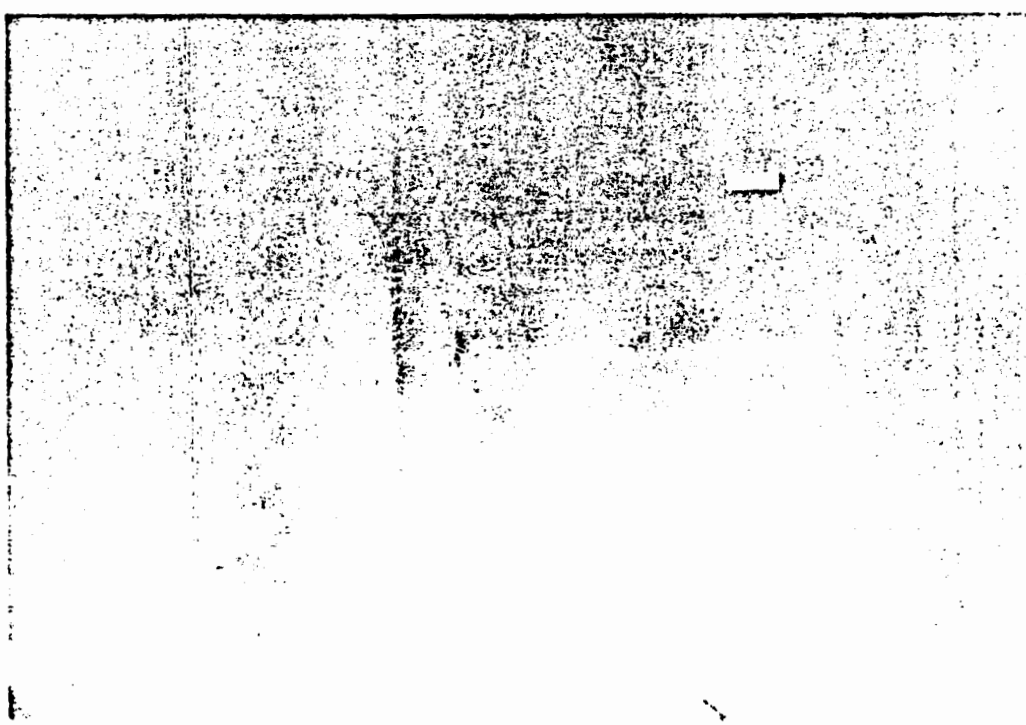

Fig. 11. Reflected light micrograph showing displacement (arrows) of a horizontal fiduciary mark at a (vertical) cement line of specimen no. 1, following 48 days creep at 37°C. Scale mark: 20 μm.

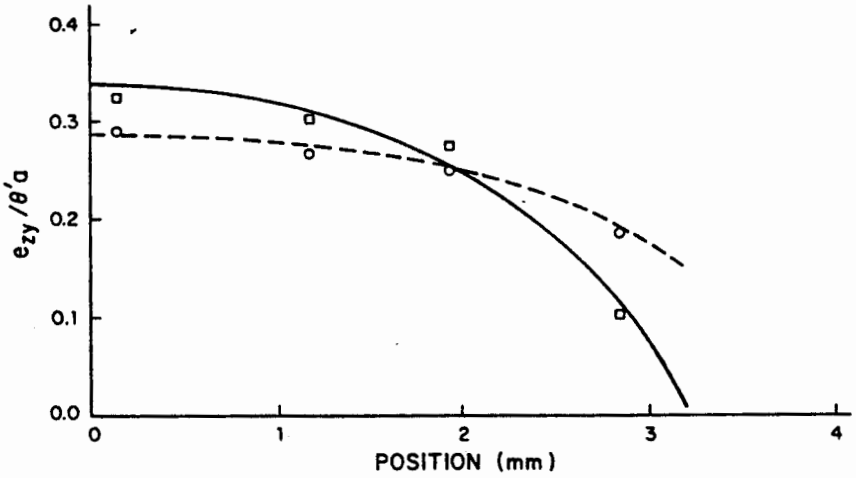

Fig. 4. Strain distribution on the boundary, human bone. Solid line: classical elasticity theory; dashed line: Cosserat elasticity theory. Circles: experiment, wet bone. Squares: experiment, dry bone.

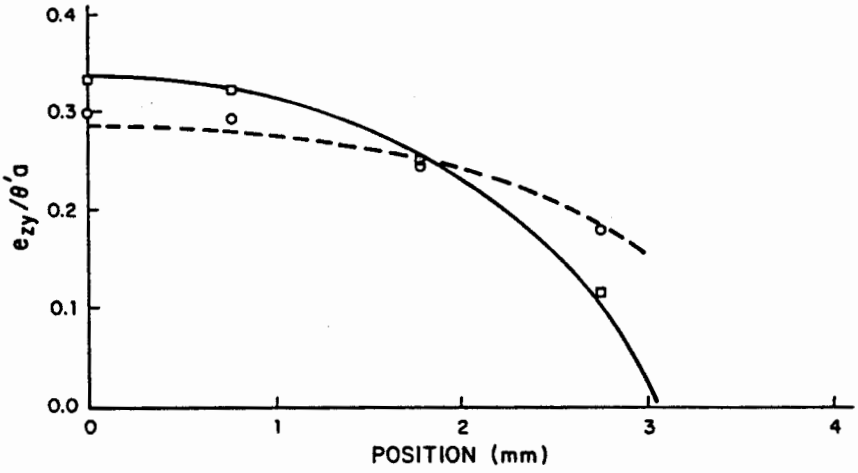

Fig. 5. Strain distribution on the boundary, human bone. Solid line: classical elasticity theory; dashed line: Cosserat elasticity theory. Circles: experiment, wet bone. Squares: experiment, dry bone.

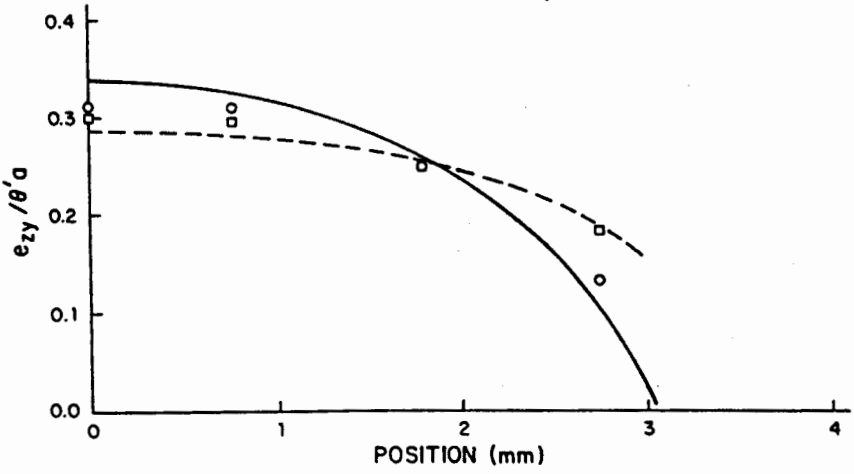

Fig. 6. Strain distribution on the boundary, human bone. Solid line: classical elasticity theory; dashed line: Cosserat elasticity theory. Squares: experiment, partly hydrated bone, 2 days in damp cloth. Circles: experiment, more fully wet bone, 4 days in damp cloth.

Table 1. Creep test data

Specimen	Applied torque (Nm)	Temperature	Period of loading	Initial strain (%)	Final creep strain† (%)	Shear modulus (GPa)*	Comments
1	0.16	37°C	131 days	0.65	0.83	3.93	
2	016	50°C	27 days	0.61	0.94	4.04	Specimen got dried
3	0.16	50°C	103 days	0.62	1.47	3.89	
4	0.19	50°C	35 days	0.56	1.10	3.53	Crack developed
5	0.30	50°C	7 days	1.22		4.84	Creep fracture
6	0.26	50°C	3 days	1.05	1.78	3.98	Crack developed
7	0.24	50°C	8 days	0.87	1.74	4.17	Crack developed
8	0.24	50°C	29 days	0.82	1.48	4.96	

* Shear moduli were calculated from 2.24×10^{-2} Nm torque (typical initial strain of 0.07%), temperature 37°C and measurement 20–40 s after loading.
† Final creep strain = (total final strain) − (initial strain).

terminating the creep test. Specimen 2 became dried unintentionally when a fluid seal leaked. Tests on specimens 1 and 3 were terminated due to time limitations. Plots of creep compliance vs time are shown in Figs 7–10. Specimens which were subjected to several experiments appear in more than one plot. In Figs 7 and 8, temperature elevation from 37 to 50°C accelerated the creep by about 5% at 1000 s and 10% at 100,000 s after loading under small torque (initial strain range 0.05–0.08%).

Despite the long period of loading, no evidence was seen in any of the specimens of the strain to approach an asymptotic value. The maximum increase in compliance during creep was about a factor of three. The creep curves disclosed nonlinear behavior: at large loads (resulting in an initial maximum shear strain of 0.6–1.2%), human bone was generally more compliant than at small loads (initial maximum strain of 0.05–0.08%).

The reflected-light micrograph in Fig. 11 shows the appearance of a specimen (No. 1) following 48 days of creep. The displacement of the fiduciary mark indicates shear slippage at the cement line. In other specimens, the cement line motion was comparable to or less than the width of the fiduciary marks (1–3 μm). Maximum cement line displacement values are listed in Table 2. The expected cement line displacement in Table 2 was computed under the supposition that all of the macroscopic shear strain (specifically, the peak classical shear strain) resulted from microdisplacements at the cement lines. Referring to Fig. 1, this strain is equivalent to $2e_{zy} = u/d$. The results in Table 2 indicate that only about one third of the macroscopic shear strain can be associated with microdisplacements at the cement lines. It proved impracticable to obtain a detailed spatial map of the microdisplacement field as in Fig. 1 or to evaluate the temporal evolution of the microdisplacements; resolution was limited by both the micro-

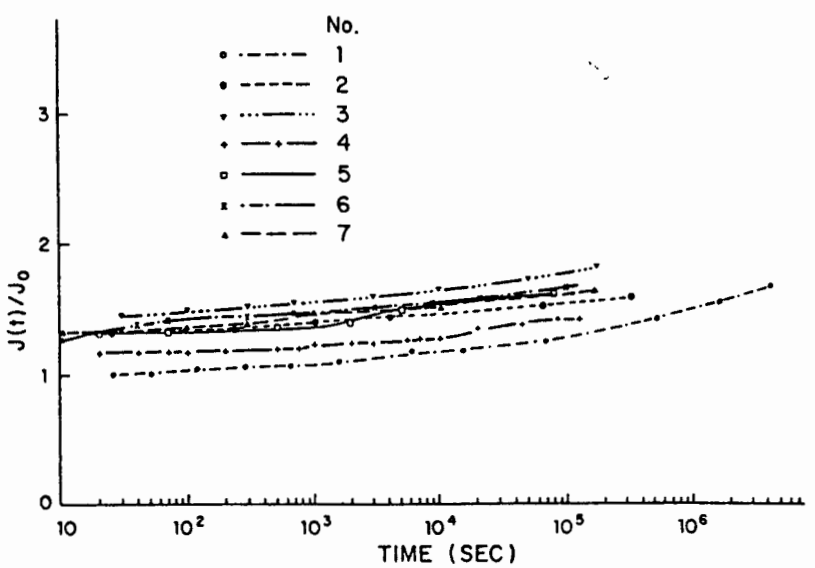

Fig. 7. Torsion creep, compact bone. Normalized compliance vs time. $1/J_0 = 3.94$ GPa. Small torque (resulting in 0.05–0.08% initial maximum shear strain), 37°C.

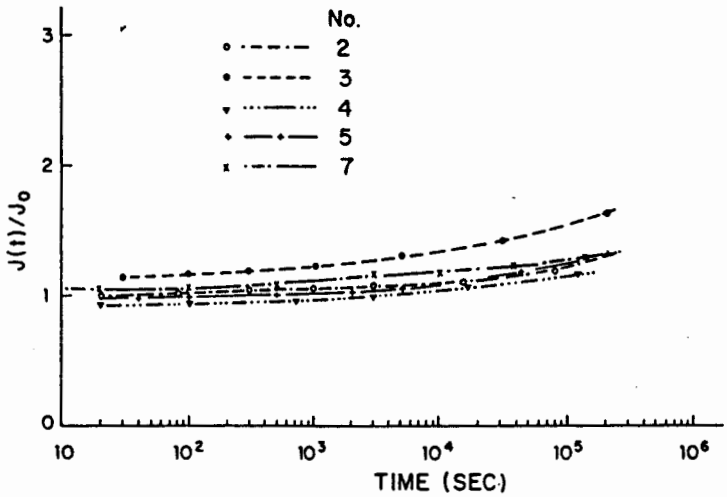

Fig. 8. Torsion creep, compact bone. Normalized compliance vs time. $1/J_0 = 3.52$ GPa. Small torque (resulting in 0.05–0.08 % initial maximum shear strain), 50°C.

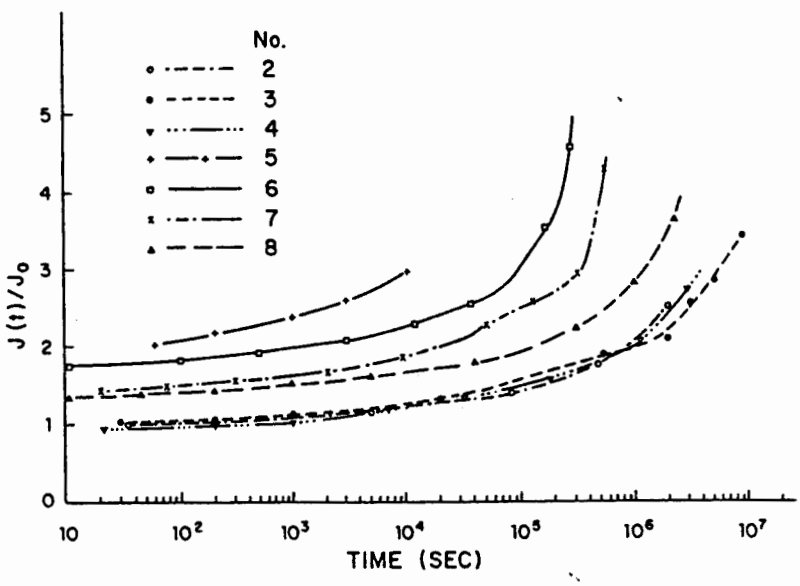

Fig. 9. Torsion creep, compact bone. Normalized compliance vs time. $1/J_0 = 3.57$ GPa. Large torque (resulting in 0.6–1.2 % initial maximum shear strain), 50°C.

scope used and the sharpness of the boundaries of the fiduciary marks.

DISCUSSION

Experimental strain distributions agreed well with the theoretical prediction for PMMA as a classical elastic medium. For bone, the strain distribution was found to be sensitive to the degree of hydration. Dry bone behaved according to the prediction of classical elasticity. Wet bone followed the prediction of Cosserat elasticity based on the elastic constants obtained using the method of size effects. Specimens of intermediate hydration exhibited nonclassical strain distributions less marked than the fully hydrated specimens.

The cause for the strain redistribution observed here is not to be found in the well-known aspects of the continuum mechanical behavior of bone. Specifically, neither plasticity nor nonlinearity can be involved since the maximum strains did not exceed 0.08 % in the strain gage experiments. At such strains in torsion, human bone was observed to deviate very little from linear behavior and to exhibit essentially complete recovery from short-term viscoelastic deformations (Lakes *et al.*, 1979). Although it is possible that microdamage occurs in bone at such strains, or that it might be introduced during the machining process, the relation between macroscopic stress and strain seems little affected. In addition, any microdamage would exist in both the wet and dry bone and hence is an unlikely source of artifact. Anisotropic effects were

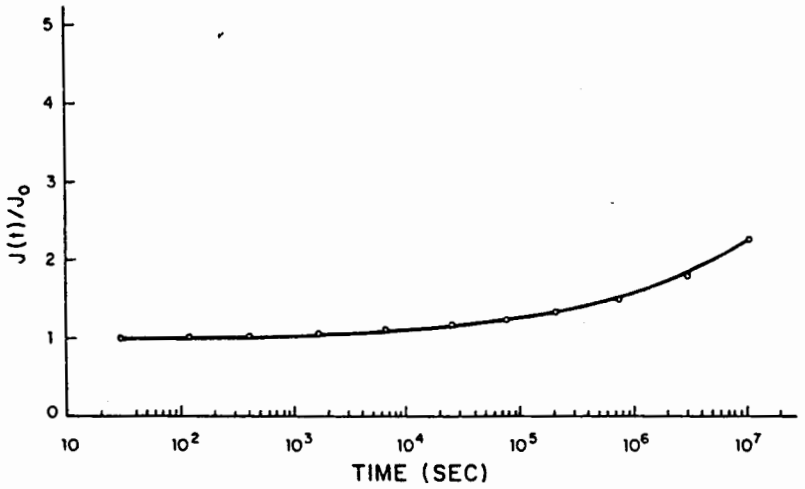

Fig. 10. Torsion creep, compact bone. Normalized compliance vs time. $1/J_0 = 3.51$ GPa. Large torque (resulting in 0.7% initial maximum shear strain), 37°C. Specimen No. 1.

Table 2. Cement line displacement due to creep

Specimen	Final creep strain (%)	Expected maximum displacement (μm)	Measured maximum displacement (μm)
1	0.83	1.45	1.0
6	1.78	4.25	0.8 ± 0.3
7	1.74	4.25	1.5 ± 0.4
8	1.48	3.70	1.5 ± 0.4

excluded by cutting the specimens in alignment with the axes of material symmetry. Viscoelastic effects were decoupled by obtaining data isochronally. The well-known hydration dependence of the elastic moduli of bone (Dempster and Liddicoat, 1959) can affect the overall magnitude of the strains resulting from a given load, but not their distribution. Strain distributions in Figs 4–6 were normalized to the twist angle per unit length so that the graphs are independent of the value of the shear modulus. Porosity gradients, hence, modulus gradients across the cortex of the bone cannot, as artifacts, cause the effects observed here since they are not dependent on the state of hydration of the bone. Specifically, a density variation from the endosteal surface to the periosteal surface of bovine femora was found by Mayer *et al.* (1983) to be associated with a modulus variation of about 8% across the cortex. This could be a potential source of error in micromechanical measurements by the method of size effects. Lakes (1981) presented arguments that such errors were not important in bone. We regard the hydration dependence observed in the present study to be much stronger evidence for the claim that porosity or modulus gradients across the cortex do not mimic micromechanical phenomena. In view of the foregoing, we consider Cosserat elasticity to be an appropriate continuum representation of wet compact bone.

The hydration dependence of the phenomena observed here may be used to evaluate hypothetical structural mechanisms for the behavior. Specifically, porous or cellular structure is predicted to give rise to micro-mechanical effects under some circumstances (Adomeit, 1967). In the case of bone any such involvement of the porosity must be small since the same pore structure is present in dry bone as in wet bone, yet dry bone behaves essentially classically. The particulate structure associated with the mineral crystallites is excluded as a mechanism for the phenomena since its size scale, tens to hundreds of Angstroms, is many orders of magnitude less than the Cosserat characteristic length found elsewhere (Yang and Lakes, 1981, 1982). The osteonal structure, by contrast, is of the correct size scale. The osteons may be regarded as stiff fibers embedded in a compliant (Katz, 1980) or viscous-like matrix (Lakes and Saha, 1979), the ground substance. Simple higher order composite theories (Hlavacek, 1975) predict generalized Cosserat elastic behavior for such a structure. The ground substance at the cement lines between osteons is a likely candidate to be the hydration-sensitive matrix by virtue of its inferred compliance, its chemical composition and morphology (Frasca, 1981) and its viscous-like behavior under prolonged stress. Further evidence for a structural role for the ground substance was provided by Frasca *et al.* (1981) who observed that single osteons

had a higher shear modulus and were less sensitive to hydration changes than microsamples containing groups of osteons.

More direct elucidation of the role of the cement substance proved elusive in this study. Although cement line motion was observed to occur in human bone, its magnitude was insufficient to permit a detailed spatial mapping of the microdisplacement field or an evaluation of the displacements as a function of time as was originally intended. The creep was observed to be accelerated less by temperature elevation than was anticipated based on the results of Lakes *et al.* (1979) and Currey (1965). Due to limitations of resolution, microdisplacements were observed only at relatively large strains and long times in creep, conditions under which bone is nonlinear. In addition, these displacements were less, typically by a factor of three, than the displacement expected if cement-line motion were the sole mechanism for the macroscopic creep. This observation contrasts with the results of Lakes and Saha (1979) in which much larger cement line displacements, more than 10 μm, were observed in young bovine plexiform bone. Creep in bovine and in human bone was comparable over a 1 day span (Lakes *et al.*, 1979), but the maximum creep strain over long time periods in human bone in this study, 0.8–1.7%, was less than values reported for bovine bone, up to 7%. In the interpretation of creep experiments of such long duration, the question of possible dissolution of bone mineral into the Ringer's solution must be considered. Lakes and Saha (1979) observed that the effects of soaking on the compliance in a long-term experiment on bovine bone (0–6%) is substantially less than the effect due to creep (100–500%) over 4 weeks duration. Yamada (1970) observed that there was almost no decrease in stiffness in human compact bone after immersion for 2 months in saline solution. These observations assure that the effects of prolonged soaking or dissolution of bone mineral represent a small perturbation on the observed time-dependent mechanical effects. In the creep experiments conducted at 50°C, an additional possibility must be considered, that of denaturation of the collagen of bone. Currey (1965) found no mechanical evidence of irreversible changes in bone up to 50°C in creep studies, and Yoon and Katz (1979) found no evidence of reversible or irreversible phase transitions in bone up to 80°C in ultrasonic studies. Regarding the comparison between young bovine bone and mature human bone, all eight specimens for the present study were obtained from a single cadaver donor, a 62 yr old male. It is possible that bone from a younger individual would behave differently, but such specimens were not available.

The results of this study have potential significance in situations in which the strain in bone varies rapidly with position. In large, whole human bones such as the femur, it is not expected that micromechanical effects will influence macroscopic stress and strain distributions very much, because strain gradients are small. Indeed, Huiskes *et al.* (1981) observed that the results of strain gage experiments upon a whole human femur were in good agreement with the predictions of classical elasticity theory. In small human bones and in the bones of small animals, however, Cosserat elastic effects may significantly alter stress distributions. In view of the present results, the size scale over which such effects are important, at least 6 mm, is considerably larger than the governing characteristic length, 0.2 mm. In addition, two situations deserve further scrutiny: (1) microcracks in bone and (2) the strength of bone with orthopaedic bone screws and wires. First, we recall that normal bone *in vivo* has microcracks (Frost, 1960; Devas, 1975). Very high stress and strain concentrations are predicted to occur near the tip of cracks in classically elastic objects under tension (Timoshenko and Goodier, 1983). In ductile materials such as various metals, local yielding near the crack tip can alleviate much of the stress concentration. Ductile materials, therefore, are less likely to break in the presence of cracks than are brittle materials. Now bone does not exhibit a great deal of ductility in comparison with, e.g. mild steel. Although one might expect bone to be excessively vulnerable to the stress concentrating effects of cracks, fracture mechanics experiments by Bonfield and Datta (1976) disclosed less susceptibility to sharp cracks than anticipated. In fracture studies, a variety of nonlinear and/or irreversible phenomena can occur near the crack tip. The present study, however, demonstrates that at small strains in the linear domain of behavior, strain in bone is redistributed away from regions where classical elasticity predicts the strain to be high, to regions where classically the strain is low. These effects, anticipated by Cosserat elasticity, can provide bone with a defense against stress concentrations associated with cracks. Cosserat elasticity, which is most likely a consequence of bone's fibrous architecture, may consequently be considered as a potential toughening mechanism. It must be distinguished from other toughening mechanisms in fibrous media which act upon moving cracks. In particular, the crack blunting mechanism of Cook and Gordon (1964) is also operative in fibrous media; this mechanism confers toughness by the action of a *weak* interface between fibers in blunting a propagating crack (see also Kelly, 1966). Evidence for the role of the cement substance as such a weak interface has been presented by Piekarski (1970). Pullout of fibers can result in a large energy absorption in the fracture of fibrous composites (Kelly, 1964). This toughening mechanism also appears to be operative in compact bone, as shown by Piekarski (1970) in micrographs of pullout of osteons in fractured bone specimens. A toughening mechanism based on Cosserat elasticity, by contrast, would depend upon reduction of the stress concentration around a crack *before* it begins to propagate. The principal mechanism for Cosserat elastic behavior in bone, as discussed earlier, appears to lie in the *compliance* of the interface between the fibers. Secondly, consider the practical

problem of strength of bone with stress raisers introduced during orthopaedic surgery. In the case of bone screws, we recall that the stress concentration for fracture around a screw hole is much less than is predicted classically. In light of the present study, this phenomenon may be viewed as consequent to the micromechanics of compact bone and its associated generalized continuum behavior, Cosserat elasticity. We have seen that nonclassical micromechanical effects can be significant over length scales comparable to the size of bone screws. It is expected that stress concentrations around such inhomogeneities could be predicted more accurately with Cosserat elasticity than with classical elasticity.

CONCLUSION

We draw the following conclusions from the results of this study.

1. Surface strain distributions in a 6 mm wide prism of wet bone differ substantially from the predictions of classical elasticity. Dry bone under the same circumstances behaves nearly classically.

2. The strain distribution in wet bone follows the prediction of Cosserat elasticity in which elastic constants determined by the method of size effects were used. Cosserat elasticity therefore has predictive power in bone mechanics.

3. The size scale over which micromechanical effects are observed, at least 6 mm, is significantly larger than the governing Cosserat characteristic length, $l_t = 0.2$ mm. This observation is consistent with the theoretical prediction.

4. The underlying physical mechanism for the Cosserat elastic effects in human compact bone is its osteonal architecture.

5. Compliance and/or viscosity of the cement substance between the osteons has been suggested as the specific mechanism involved. Cement line motion under prolonged load in mature human bone appears, however to be less pronounced than in (immature) bovine plexiform bone.

Acknowledgements—This paper is based on part of a dissertation submitted by H. C. Park in partial fulfillment of the requirements of the Ph.D. in Mechanical Engineering. A portion of the results were presented at the ASME Biomechanics Symposium, Albuquerque, NM, U.S.A., June 1985. The authors thank Professor Y. K. Liu and D. V. Lakes for their encouragement and for critiques of the manuscript.

REFERENCES

Achenbach, J. D. (1976) Generalized continuum theories for directionally reinforced solids. *Archs Mech., Warsaw* **28**, 257–278.

Adomeit, G. (1967) Determination of elastic constants of a structured material. *Mechanics of Generalized Continua* (Edited by Kroner, E.), IUTAM Symposium, Freudenstadt, Stuttgart, Springer, Berlin.

Askar, A. and Cakmak, A. S. (1968) A structural model of a micropolar continuum. *Int. J. Engng Sci.* **6**, 583–589.

Bonfield, W. and Datta, P. K. (1976) Fracture toughness of compact bone. *J. Biomechanics* **9**, 131–134.

Bonfield, W. and Grynpas, M. D. (1977) Anisotropy of Young's modulus of bone. *Nature* **270**, 453–454.

Brooks, D. B., Burstein, A. H. and Frankel, V. H. (1970) The biomechanics of torsional fracture. *J. Bone Jt. Surg.* **52A**, 507–514.

Carter, D. R., Caler, W. E., Spengler, D. M. and Frankel, V. H. (1981) Uniaxial fatigue of human cortical bone. The influence of tissue physical characteristics. *J. Biomechanics* **14**, 461–470.

Cook, J. and Gordon, J. E. (1964) A mechanism for the control of crack propagation in all-brittle systems. *Proc. R. Soc.* **A282**, 508–520.

Cowin, S. C. (1970) An incorrect inequality in micropolar elasticity theory. *J. appl. Math. Phys. (ZAMP)* **21**, 494–497.

Currey, J. D. (1965) Anelasticity in bone and echinoderm skeletons. *J. exp. Biol.* **43**, 279–292.

Dempster, W. and Liddicoat, R. (1959) Compact bone as a non-isotropic material. *Am. J. Anat.* **91**, 331–362.

Devas, M. B. (1975) *Stress Fractures.* Churchill Livingston, London.

Ellis, R. W. and Smith, C. W. (1968) A thin-plate analysis and experimental evaluation of couple-stress effects. *Exp. Mech.* **7**, 372–380.

Ejike, U. B. C. O. (1969) The plane circular crack problem in the linearized couple-stress theory. *Int. J. Engng Sci.* **7**, 947–961.

Eringen, A. C. (1967) Linear theory of micropolar viscoelasticity. *Int. J. Engng Sci.* **5**, 191–204.

Eringen, A. C. (1968) Theory of micropolar elasticity. *Fracture* Vol. 2 (Edited by Liebowitz, H.), pp. 621–729. Academic Press, New York.

Frasca, P. (1981) Scanning-electron microscopy studies of 'ground substance' in the cement lines, resting lines, hypercalcified rings, and reversal lines of human cortical bone. *Acta. Anat.* **109**, 115–121.

Frasca, P., Harper, R. and Katz, J. L. (1981) Strain and frequency dependence of shear storage modulus for human single osteons and cortical bone microsamples-size and hydration effects. *J. Biomechanics* **14**, 679–690.

Frost, H. M. (1960) Presence of microscopic cracks *in vivo* in bone. *Henry Ford Hosp. med. Bull* **8**, 27–35.

Gauthier, R. D. and Jahsman, W. E. (1975) A quest for micropolar elastic constants. *J. appl. Mech.* **42**, 369–374.

Hlavacek, M. (1975) A continuum theory for fibre reinforced composites. *Int. J. Solids Structures* **11**, 199–211.

Huiskes, R., Janssen, J. D. and Slooff, T. J. (1981) A detailed comparison of experimental and theoretical stress analyses of a human femur. *Mechanical Properties of Bone*, Joint ASME-ASCE Applied Mechanics, Fluids Engineering and Bioengineering Conference, Boulder, Colorado. ASME, New York.

Katz, J. L. (1980) Anisotropy of Young's modulus of bone. *Nature* **283**, 106–107.

Kelly, A. (1964) The strengthening of metals by dispersed particles. *Proc. R. Soc.* **A282**, 63–79.

Kelly, A. (1966) *Strong Solids.* Oxford University Press, London.

Kim, B. S. and Eringen, A. C. (1973) Stress distribution in an elliptic hole in an infinite micropolar elastic plate. *Lett. appl Engng Sci.* **1**, 381–390.

Lakes, R. S. (1981) Dynamical study of couple stress effects in human compact bone. *J. biomech. Engng* **104**, 6–11.

Lakes, R. S. and Saha, S. (1979) Cement line motion in bone. *Science* **204**, 501–503.

Lakes, R. S., Katz, J. L. and Sternstein, S. S. (1979) Viscoelastic properties of wet cortical bone–I. Torsional and biaxial studies. *J. Biomechanics* **12**, 657–678.

Lakes, R. S. and Yang, J. F. C. (1983a). Concentration of strain around holes in a strip of compact bone, *Develop. Mech.* **12**, 233–237 (Proceedings of the 18th Midwestern Mechanics Conference, Iowa City, 16 May 1983).

Lakes, R. S. and Yang, J. F. C. (1983b) Cosserat elasticity in bone: rotation modulus κ. *Develop. Mech.* **12**, 239–242 (Proceedings of the 18th Midwestern Mechanics Conference, Iowa City, 16 May 1983).

Lakes, R. S. (1986) Experimental microelasticity of two porous solids. *Int. J. Solids Structures* **22**, 55–63.

Lanyon, L. E., Hampson, W. G., Goodship, A. E. and Shah, J. S. (1975) Bone deformation recorded *in vivo* from strain gages attached to the human tibial shaft. *Acta orthop. scand.* **46**, 256–268.

Malcolm, D. J. (1982) Orthogonal fibre composites as micromorphic materials. *Int. J. Engng Sci.* **20**, 1111–1124.

Mindlin, R. D. and Tiersten, H. F. (1962) Effects of couple stresses in linear elasticity. *Archs Ration. Mech. Analysis* **11**, 415–448.

Mayer, D. C., Ashman, R. B., Cowin, S. C. and Van Buskirk, W. C. (1983) Radial variations in the elastic properties of bovine cortical bone. *Transactions of the 29th Annual Meeting of the Orthopaedic Research Society* Vol. 8, p. 284. ORS, Chicago.

Park, H. C. and Lakes, R. S. (in press) Torsion of a micropolar elastic prism of square cross section.

Perry, C. C. and Lissner, H. R. (1962) *The Strain Gage Primer*. McGraw-Hill, New York.

Piekarski, K. (1970) Fracture of bone. *J. appl. Phys.* **41**, 215–223.

Schijve, J. (1966) Note on couple stresses. *J. Mech. Phys. Solids* **14**, 113–120.

Timoshenko, S. P. and Goodier, J. N. (1983) *Theory of Elasticity*, 3rd edn. McGraw-Hill, New York.

Wright, T. M., Barnett, D. M. and Hayes, W. C. (1977) Residual stresses in bone. *Recent Advances in Engineering Science* Vol. 3. Scientific Publishers, Boston. (Proceedings 10th meeting, Society of Engineering Science, Raliegh, NC, 1973), pp. 25–32. Scientific Publishers, Boston.

Yamada, H. (1970) *Strength of Biological Materials*. Williams & Wilkins, Baltimore.

Yang, J. F. C. and Lakes, R. S. (1981) Transient study of couple stress effects in human compact bone: Torsion. *J. biomech. Engng* **103**, 275–279.

Yang, J. F. C. and Lakes, R. S. (1982) Experimental study of micropolar and couple stress elasticity in compact bone in bending. *J. Biomechanics* **15**, 91–98.

Yoon, H. S. and Katz, J. L. (1979) Temperature dependence of the ultrasonic velocities in bone. 1979 *Ultrasonics Symposium Proceedings*. IEEE.

APPENDIX A: CONSTITUTIVE EQUATIONS FOR COSSERAT ELASTICITY

The constitutive equations of linear isotropic micropolar elasticity, considered to be identical to Cosserat elasticity are (Eringen, 1968)

$$\sigma_{kl} = \lambda e_{rr}\delta_{kl} + (2\mu+\kappa)e_{kl} + \kappa\varepsilon_{klm}(r_m - \phi_m)$$

$$m_{kl} = \alpha\phi_{r,r}\delta_{kl} + \beta\phi_{k,l} + \gamma\phi_{l,k}$$

in which the usual Einstein summation convention is used and the comma denotes differentiation with respect to spatial variables. e_{kl} is the usual small strain tensor, defined in terms of the displacement u: $e_{kl} = 1/2(u_{k,l} + u_{l,k})$; r_m is the macrorotation $r_m = 1/2\ \varepsilon_{mln}u_{n,l}$ in which ε is the permutation symbol, σ_{kl} is the asymmetric force stress tensor, m_{kl} is the couple stress tensor and ϕ is the microrotation vector, which is kinematically independent of the macrorotation, r. The quantities λ, μ, κ, α, β, γ are Cosserat elastic constants. Thus the isotropic Cosserat solid has six elastic constants, in contrast to the classically elastic solid which has two. The classical solid is obtained as a special case of the Cosserat solid when α, β, γ, and κ are zero.

The following combinations of elastic constants have physical significance and may be referred to as technical constants.

Young's modulus (Nm^{-2})

$$E = (2\mu+\kappa)(3\lambda+2\mu+\kappa)/(2\lambda+2\mu+\kappa)$$

Shear modulus (Nm^{-2})

$$G = (2\mu+\kappa)/2$$

Poisson ratio (dimensionless)

$$\nu = \lambda/(2\lambda+2\mu+\kappa)$$

Characteristic length, torsion (m)

$$l_t = [(\beta+\gamma)/(2\mu+\kappa)]^{1/2}$$

Characteristic length, bending (m)

$$l_b = [\gamma/2(2\mu+\kappa)]^{1/2}$$

Coupling number (dimensionless)

$$N = [\kappa/2(\mu+\kappa)]^{1/2}$$

Polar ratio (dimensionless)

$$\psi = (\beta+\gamma)/(\alpha+\beta+\gamma).$$

APPENDIX B: THEORETICAL STRAIN DISTRIBUTION

The solution of a boundary value problem of torsion of a square cross sectional prism in linear isotropic Cosserat elasticity theory was obtained by Park and Lakes (in press). According to the solution, shear strain distributions on the lateral surfaces are different from those of classical elasticity theory. The shear strain e_{zy} depends on the Cosserat elastic coefficients of the medium as follows

$$e_{zy}|_{x=a/2} = \theta\{2(1+C)a - \sum_{n=0}^{\infty}\frac{8}{ak_n^2\cosh(k_n a/2)}\cosh(k_n y) - \sum_{n=0}^{\infty} CA_n p_n(-1)^n\cosh(p_n y) + \sum_{n=0}^{\infty} CA_n k_n \sinh(p_n a/2)\cos(k_n y)\} \quad (1)$$

where

$$k_n = (2n+1)\pi/a,\ p_n = [k_n^2 - (N/l_b)^2]^{1/2},\quad C = 25\,Nl_t/a,$$

$$A_n = \frac{8(-1)^n(1-N^2)}{ak_n^2 p_n\cosh(p_n a/2)} - \frac{4(-1)^n N^2 l_t^2\tanh(k_n a/2)/l_b^2 k_n + (l_t^2/2l_b^2 - 1)8(-1)^n\psi C\tanh(p_n a/2)/p_n}{Ca[(p_n^2 + l_t^2/2l_b^2 - 1)(1-\psi)k_n^2]\sinh(p_n a/2)},$$

and a is the width of the prism and the angle of twist per unit length is $\theta(1+C)$. l_t, l_b, N and ψ are the Cosserat characteristic lengths, coupling number and polar ratio, respectively.

In the present study, the above analytical solution was used as the basis of new experiments upon compact bone.